Supplementary Information

Efficient symmetric oligomer hole conductors with different cores for high performance perovskite solar cells

Hyeju Choi,[a] Sojin Park,[a] Moon-Sung Kang,[b] Jaejung Ko [*,a]

[a] *Department of Advanced Material Chemistry, Korea University Sejong Campus, Sejong-ro 2511, Sejong City, 339-700, Korea. Fax: +82-41-867-1331; Tel: +82-41-860-1337; E-mail: jko@korea.ac.kr*

[c] *Department of Environmental Engineering, Sangmyung University, 300 Anseo-dong, Dongnam-gu, Cheonan-si, Chungnam 330-720, Republic of Korea*

1. Materials and HTM synthesis

Most reactions were performed under a nitrogen atmosphere. All reagents were purchased from commercial suppliers such as Sigma-Aldrich, Alfa, and TCI. 4-Methoxy-*N*-(4-methoxyphenyl)-*N*-(4-(4,4,5,5-tetramethyl-1,3,2-dioxaborolan-2-yl)phenyl)aniline,[1] 5,7-bis(4-bromophenyl)-2,3-dihydrothieno[3,4-*b*][1,4]dioxine,[2] and 4,7-bis(4-

bromophenyl)benzo[*c*][1,2,5]thiadiazole[2] were synthesized using a procedure of previous literature.

^{1}H and ^{13}C NMR spectra were recorded on a Varian Mercury 300 spectrometer. Chemical shifts δ were calibrated against TMS as an internal standard. Elemental analyses were performed with a Carlo Elba Instruments CHNS-O EA 1108 analyzer. The absorption and photoluminescence spectrometer were recorded on a Perkin-Elmer Lambda 2S UV-visible spectrometer and Perkin LS fluorescence, respectively.

Cyclic voltammetry was carried out with a BAS 100B (Bioanalytical Systems, Inc.). Redox potential of materials was measured in dichloromethane solution with 0.1 M $(n\text{-}C_4H_9)_4NPF_6$ as the supporting salt. The platinum working electrode consisted of a platinum wire sealed in a soft glass tube with a surface of 0.785 mm^2, which was polished down to 0.5 μm with Buehler polishing paste prior to use in order to obtain reproducible surfaces. The counter electrode consisted of a platinum wire and the reference electrode was an Ag/AgCl secondary electrode.

N^4-(4'-(Bis(4-methoxyphenyl)amino)biphenyl-4-yl)-$N^{4'}$,$N^{4'}$-bis(4-methoxyphenyl)biphenyl-4,4'-diamine (1). 4-Methoxy-*N*-(4-methoxyphenyl)-*N*-(4-(4,4,5,5-tetramethyl-1,3,2-dioxaborolan-2-yl)phenyl)aniline (2 g, 4.64 mmol), potassium carbonate (1.44 g, 1.04 mmol), $Pd(PPh_3)_4$ (0.15 g, 0.13 mmol) and water (2 mL) were added to a solution of bis(4-bromophenyl)amine (0.68 g, 2.08 mmol) in THF (20 mL) in a Schlenk tube. The Schlenk tube was degassed and the mixture was stirred at reflux under an argon atmosphere for overnight. The cooled mixture was then extracted with diethyl ether and the extracts were washed with brine and dried Magnesium sulfate. The solvent was removed in vacuo and the residue was purified by column chromatography on silica gel eluting with CH_2Cl_2/Hexane (1:1) to give compound **1**. (1 g, 1.29 mmol, 62%) ^{1}H NMR (300 MHz, CD_2Cl_2): δ 7.47 (d, 8H, J = 8.7 Hz), 7.38 (d, 8H, J = 8.7 Hz), 7.12 (d, 8H, J = 9.0 Hz), 7.04 (d, 16H, J = 9.0 Hz), 6.93 (d, 8H, J = 8.7 Hz), 6.83 (d, 16H, J = 9.0 Hz), 5.9 (s, 1H), 3.75 (s, 24H). ^{13}C NMR (75 MHz, CD_2Cl_2): δ 156.3, 148.0, 142.2, 141.3, 133.7, 133.1, 127.5, 127.1, 126.8, 121.2, 118.2, 115.0, 55.8. MS: *m/z* 775.34 [M^+]. Anal. Calcd. for $C_{52}H_{45}N_3O_4$: C, 80.49; H, 5.85. . Found: C, 80.14; H, 5.48.

N^4,$N^{4'}$-(Biphenyl-4,4'-diyl)bis(N^4-(4'-(bis(4-methoxyphenyl)amino)biphenyl-4-yl)-$N^{4'}$,$N^{4'}$-bis(4-methoxyphenyl)biphenyl-4,4'-diamine) (B[BMPDP]$_2$). To a two-necked flask equipped with a stopcock and a condenser were added 4,4'-Diiodobiphenyl (0.08 g, 0.2 mmol), compound **1** (0.37 g, 0.48 mmol), sodium *tert*-butoxide (0.06 g, 0.62 mmol), and dry toluene (10 mL) under nitrogen atmosphere. Then, $Pd_2(dba)_3$ (0.01 g, 0.01 mmol), and *tri-tert*-butylphosphine (0.1 eq) was added to the flask, and the mixture was stirred at reflux for overnight. After cooling to room temperature, the mixture was then extracted with dichloromethane and the extracts were washed with brine and dried $MgSO_4$. The solvent was removed in vacuo and the residue was purified by column chromatography yielded the product as a yellow solid. Yield: 65%. ^{1}H NMR (300 MHz, CD_2Cl_2): δ 7.46-7.52 (dd, 12H, J = 9.0 Hz), 7.40 (d, 8H, J = 9.0 Hz), 7.15 (d, 12H, J = 8.7 Hz), 7.05 (d, 16H, J = 8.7 Hz), 6.93 (d, 8H, J = 8.7 Hz), 6.83 (d, 16H, J = 9.0 Hz), 3.8 (s, 24H). ^{13}C NMR (75 MHz, CD_2Cl_2): δ 156.5, 148.3, 147.0, 146.6, 141.3, 135.7, 135.2, 132.8, 127.7, 127.5, 127.4, 127.0, 124.9, 124.6, 121.1, 115.1, 55.8. MS: *m/z* 1701.73 [M^+]. Anal. Calcd. for $C_{116}H_{96}N_6O_8$: C, 81.86; H, 5.69. Found: C, 81.48; H, 5.47.

N^4,$N^{4'}$-(4,4'-(2,3-Dihydrothieno[3,4-b][1,4]dioxine-5,7-diyl)bis(4,1-phenylene))bis(N^4-(4'-(bis(4-methoxyphenyl)amino)biphenyl-4-yl)-$N^{4'}$,$N^{4'}$-bis(4-methoxyphenyl)biphenyl-4,4'-diamine) (DPEDPT-B[BMPDP]$_2$). The product **DPEDPT-B[BMPDP]$_2$** was prepared using the same procedure for **B[BMPDP]$_2$** except that 5,7-bis(4-bromophenyl)-2,3-dihydrothieno[3,4-*b*][1,4]dioxine (0.1 g, 0.22 mmol) were used instead of 4,4'-Diiodobiphenyl. Yield: 72%. ^{1}H NMR (300 MHz, CD_2Cl_2): δ 77.63 (d, 4H, J = 8.1 Hz), 7.46 (d, 8H, J = 9.0 Hz), 7.40 (d, 8H, J = 8.7 Hz), 7.14 (d, 8H, J = 8.1 Hz), 7.10 (d, 4H, J = 8.7 Hz), 7.05 (d, 16H, J = 8.7 Hz), 6.93 (d, 8H, J = 8.7 Hz), 6.83 (d, 16H, J = 9.0 Hz), 4.3 (s, 4H), 3.8 (s, 24H). ^{13}C NMR (75 MHz, CD_2Cl_2): δ 156.5, 148.3, 146.5, 146.4, 141.3, 138.7, 135.7, 132.8, 127.8, 127.5, 127.4, 127.1, 127.0, 124.9, 124.2, 121.1, 115.1, 65.2, 55.8. MS: *m/z* 1841.73 [M^+]. Anal. Calcd. for $C_{122}H_{100}N_6O_{10}S$: C, 79.54; H, 5.47. Found: C, 79.22; H, 5.32.

N^4,$N^{4'}$-(4,4'-(Benzo[*c*][1,2,5]thiadiazole-4,7-diyl)bis(4,1-phenylene))bis(N^4-(4'-(bis(4-methoxyphenyl)amino)biphenyl-4-yl)-$N^{4'}$,$N^{4'}$-bis(4-methoxyphenyl)biphenyl-4,4'-diamine) (DPBTD-B[BMPDP]$_2$). The product **DPBTD-B[BMPDP]$_2$** was prepared using the same procedure for **B[BMPDP]$_2$** except that 4,7-bis(4-bromophenyl)benzo[*c*][1,2,5]thiadiazole (0.1 g,

0.22 mmol) were used instead of 4,4'-Diiodobiphenyl. Yield: 68%. ^{1}H NMR (300 MHz, CD_2Cl_2): δ 7.91 (d, 4H, J = 8.1 Hz), 7.76 (s, 2H), 7.49 (d, 8H, J = 9.0 Hz), 7.41 (d, 8H, J = 8.7 Hz), 7.21-7.27 (dd, 12H, J = 9.0 Hz), 7.05 (d, 16H, J = 8.7 Hz), 6.94 (d, 8H, J = 8.7 Hz), 6.83 (d, 16H, J = 9.0 Hz), 3.79 (s, 24H). ^{13}C NMR (75 MHz, CD_2Cl_2): δ 156.5, 154.6, 148.4, 148.2, 146.4, 141.3, 136.1, 132.7, 132.4, 131.7, 130.4, 127.8, 127.6, 127.4, 127.0, 125.4, 123.4, 121.1, 115.1, 55.9. MS: *m/z* 1835.73 [M^+]. Anal. Calcd. for $C_{122}H_{98}N_8O_8S$: C, 79.80; H, 5.38. Found: C, 79.54; H, 5.27.

Reference

[1] L. Yu, J. Xi, H. T. Chan, T. Su, L. J. Antrobus, B. Tong, Y. Dong, W. K. Chan, D. L. Phillips, *J. Phys. Chem. C* 2013, **117**, 2041-2052.

[2] K. Tsuchiya, T. Sakakura, K. Ogino, *Macromolecules* 2011, **44**, 5200-5208.

2. Solar cell fabrication

F-doped tin oxide (FTO) glass plates (Pilkington, TEC-8) were cleaned in a detergent solution using an ultrasonic bath for 30 min, rinsed with water and ethanol. The compact TiO_2 layer was deposited on the etched FTO substrate by spray pyrolysis at 450 ^{o}C, using titanium diisopropoxide bis(acetylacetonate) solution. The FTO glass plates were immersed in 40 mM $TiCl_4$ aqueous solution at 70 ^{o}C for 30 min and then sintered at 500 ^{o}C for 30 min. Mesoporous TiO_2 films was deposited by spin coating of a diluted TiO_2 paste (Dyesol 18NR-T, 1:3.5 w/w diluted with ethanol) at 5000 rpm for 30 s. The films were successively sintered at 500 ^{o}C. The PbI_2 in DMF solution (1.0 M) was dropped on the TiO_2/FTO substrate and then spin-coated at 6500 rpm for 30 s and dried on a hot plate at 70 ^{o}C for 30 min. After cooling down, the film was dipped into a CH_3NH_3I/2-propanol solution (8 mg/mL) for 25 s, and dried at 70 ^{o}C for 15 min. For a deposition of HTM layers, HTM/chlorobenzene (30 mM) solutions were prepared with two additives. 3.5 μL lithium bis(trifluoromethanesulonyl)imide (Li-TFSI)/acetonitrile (520 mg/1 mL) and 8.0 μL (4-*tert*-butylpyridine) (TBP) were added to the HTM/chlorobenzene solutions as additives. The HTMs were spin-cast on top of the $CH_3NH_3PbI_3$/TiO_2/FTO substrate at 3000 rpm. Finally, the device was pumped

down to lower than 10^{-5} torr and a ~60 nm thick Au counter electrode was deposited on top.

3. Solar cell performance measurement

Solar cell efficiencies were evaluated under simulated one sun irradiation from a Xe arc lamp with an AM 1.5 global filter. Irradiance was characterized using a calibrated spectrometer and illumination intensity was set using an NREL certified silicon diode with an integrated KG1 optical filter: spectral mismatch factors were calculated for each device in this report to be less than 5%. Short circuit currents were also found to be with 5% of values calculated using the integrated external quantum efficiency (EQE) spectra and the solar spectrum. The EQE was measured by under filling the device area using a reflective microscope objective to focus the light output from a 75 watt Xe lamp, monochromator, and optical chopper; photocurrent was measured using a lock-in amplifier and the absolute photon flux was determined by a calibrated silicon photodiode.

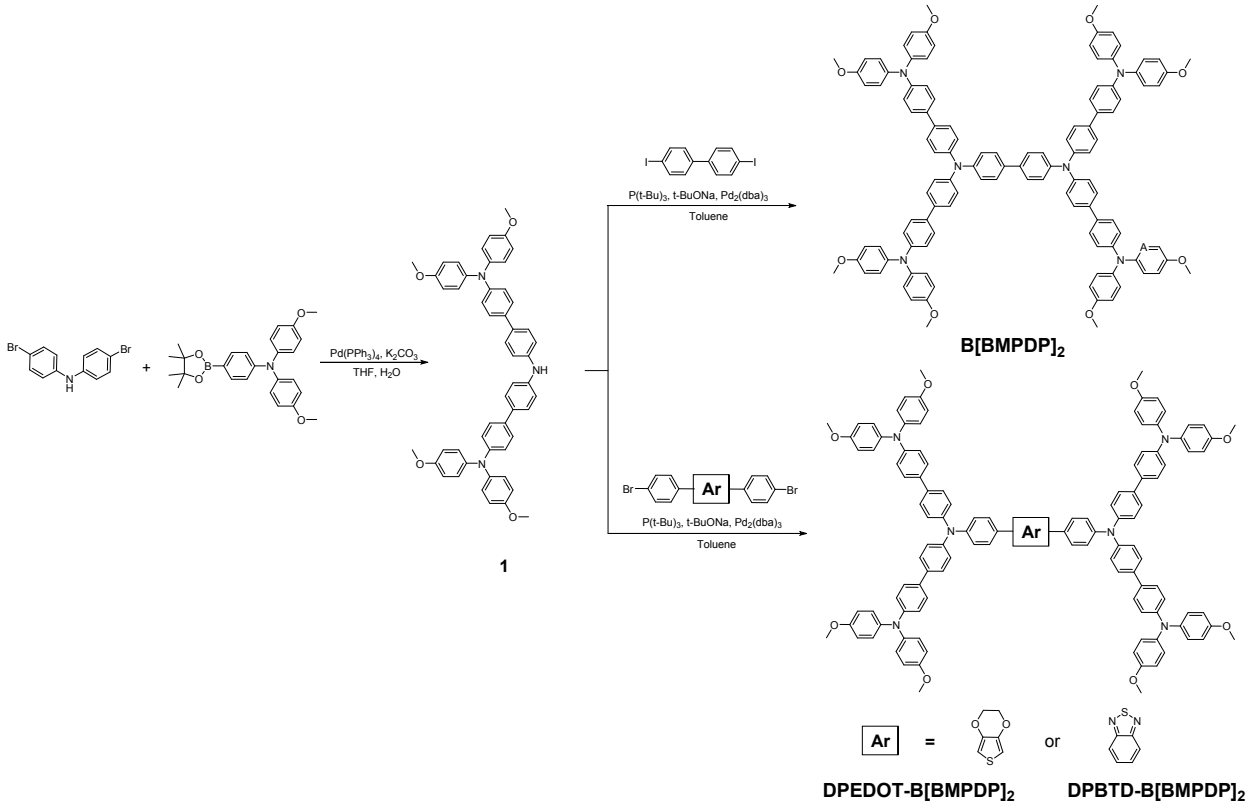

Figure S1. Schematic diagram for the synthesis of the **B[BMPDP]$_2$**, **DPEDOT-B[BMPDP]$_2$** and **DPBTD-B[BMPDP]$_2$**.

Table S1. Optical, redox parameters of the compounds

Compounds	λ_{abs}[a]/nm (ε/M^{-1}cm^{-1})	λ_{PL}[a]/nm	HOMO (eV)[b]	LUMO (eV)[c]	E_{gap} (eV)[d]
B[BMPDP]$_2$	376 (157,500)	429	-5.33	-2.33	3.00
DPEDOT-B[BMPDP]$_2$	377 (152,000)	472	-5.22	-2.55	2.67
DPBTD-B[BMPDP]$_2$	473 (24,600)	648	-5.34	-2.96	2.38

[a] UV-vis absorption spectra and fluorescence spectra were measured in chlorobenzene solution. [b] Redox potential of the compounds were measured in CH_2Cl_2 with 0.1M (n-$C_4H_9)_4NPF_6$ with a scan rate of 100 mVs^{-1} (*vs*. Fc/Fc$^+$). [c] E_{LUMO}= E_{HOMO} + E_{gap}. [d] E_{gap} was calculated from the absorption thresholds from absorption spectra.

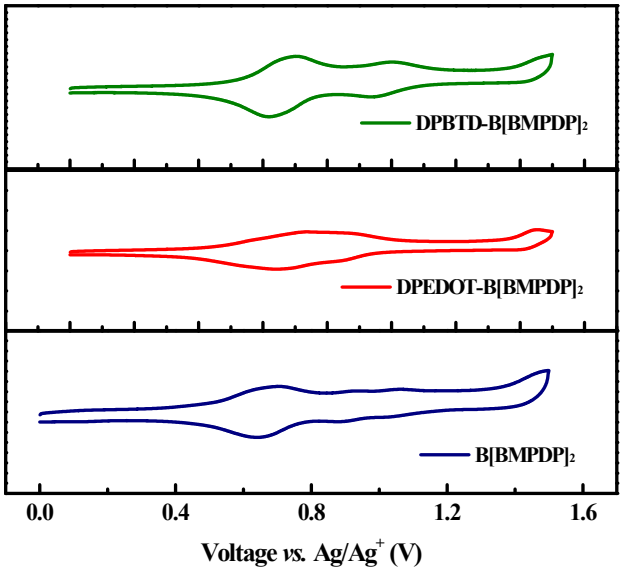

Figure S2. Electrochemical characterization of the **B[BMPDP]$_2$**, **DPEDOT-B[BMPDP]$_2$**, and **DPBTD-B[BMPDP]$_2$** in dichloromethane/(n-$C_4H_9)_4NPF_6$ (0.1 M) with a scan speed of 100 mV/s.

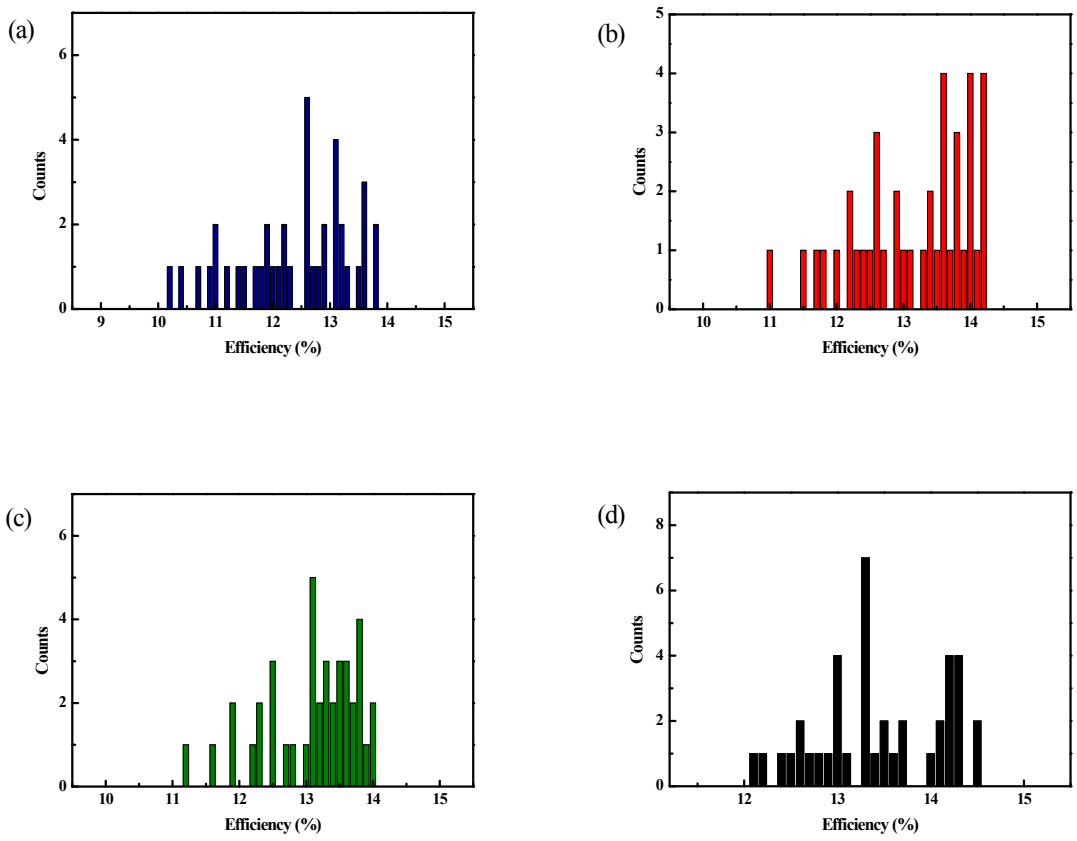

Figure S3. Histogram of the solar cell efficiencies obtained from the (a) **B[BMPDP]$_2$**, (b) **DPEDOT-B[BMPDP]$_2$**, (c) **DPBTD-B[BMPDP]$_2$** and (d) **spiro-OMeTAD** based hybrid solar cells.

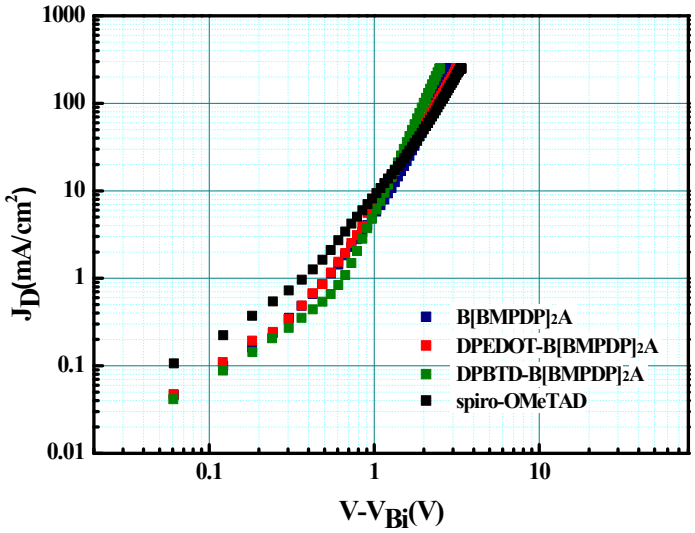

Figure S4. Space charge limitation of current *J-V* characteristics of the HTMs.

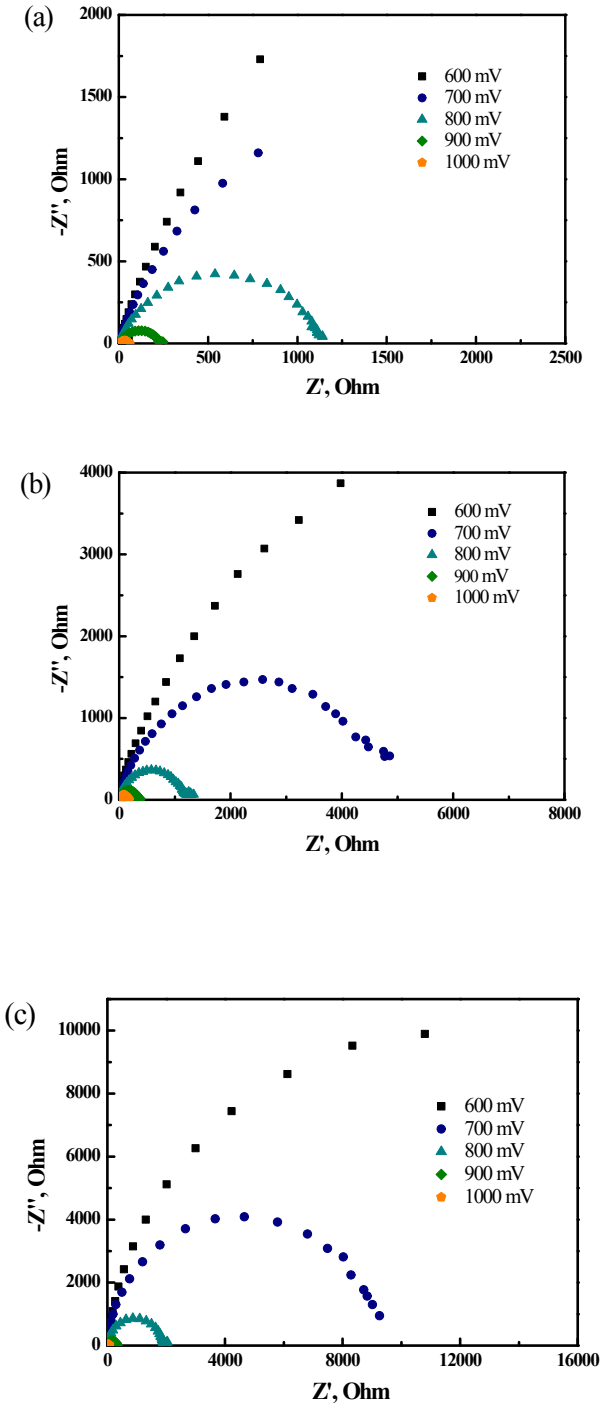

Figure S5. Nyquist plots of the devices with (a) **B[BMPDP]$_2$**, (b) **DPEDOT-B[BMPDP]$_2$** and (c) **DPBTD-B[BMPDP]$_2$** measured in the dark over different forward biases.

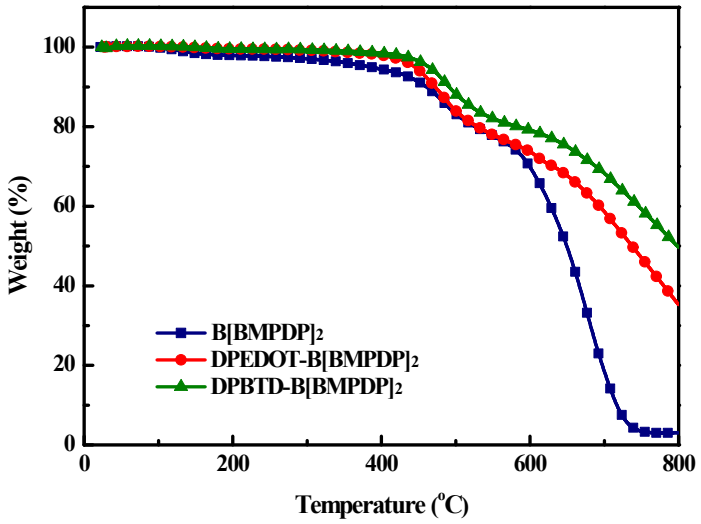

Figure S6. Thermo-gravimetric analysis of the HTMs.

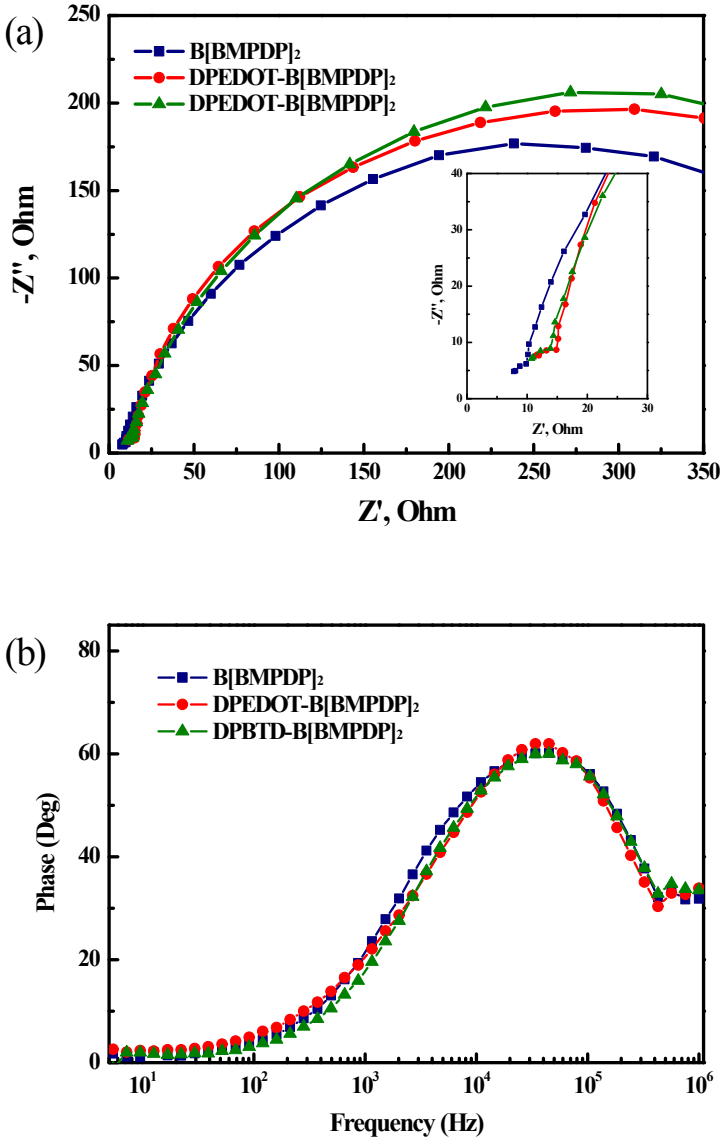

Figure S7. (a) Nyquist plots and (b) Bode phase plots measured in dark conditions at a forward bias of -0.85 V. The inset is the zoom of the low impedance region.